Understanding the plasmonic properties of dewetting formed Ag nanoparticles in large area solar cell applications

Article *in* Optics Express · July 2013

DOI: 10.1364/OE.21.018344

CITATIONS
20

READS
136

6 authors, including:

Irem Tanyeli
Chalmers University of Technology
9 PUBLICATIONS **115** CITATIONS
SEE PROFILE

Gürsoy b Akgüç
Izmir Ekonomi Üniversitesi
35 PUBLICATIONS **197** CITATIONS
SEE PROFILE

Alpan Bek
Middle East Technical University
66 PUBLICATIONS **936** CITATIONS
SEE PROFILE

Oguz Gülseren
Bilkent University
140 PUBLICATIONS **3,421** CITATIONS
SEE PROFILE

Understanding the plasmonic properties of dewetting formed Ag nanoparticles for large area solar cell applications

M. Can Günendi,[1] İrem Tanyeli,[2,3,4] Gürsoy B. Akgüç,[1,*] Alpan Bek,[2,3] Raşit Turan,[2,3] and Oğuz Gülseren[1]

[1]*Department of Physics Bilkent University, Bilkent 06800 Ankara, Turkey*
[2]*Department of Physics, Middle East Technical University, Dumlupinar Blvd. 1, Cankaya 06800 Ankara, Turkey*
[3]*Center for Solar Energy Research and Applications, Middle East Technical University, Dumlupinar Blvd. 1, Cankaya, Ankara 06800, Turkey*
[4]*Currently with the Dutch Institute for Fundamental Energy Research, Trilateral Euregio Cluster, 3430 BE Nieuwegein, The Netherlands*
[*]*gursoy@fen.bilkent.edu.tr*

Abstract: The effects of substrates with technological interest for solar cell industry are examined on the plasmonic properties of Ag nanoparticles fabricated by dewetting technique. Both surface matching (boundary element) and propagator (finite difference time domain) methods are used in numerical simulations to describe plasmonic properties and to interpret experimental data. The uncertainty on the locations of nanoparticles by the substrate in experiment is explained by the simulations of various Ag nanoparticle configurations. The change in plasmon resonance due to the location of nanoparticles with respect to the substrate, interactions among them, their shapes, and sizes as well as dielectric properties of substrate are discussed theoretically and implications of these for the experiment are deliberated.

OCIS codes: (240.6680) Surface plasmons; (250.5403) Plasmonics; (350.6050) Solar energy; (310.7005) Transparent conductive coatings.

References and Links

1. H. A. Atwater and A. Polman, "Plasmonics for improved photovoltaic devices," Nat. Mater. **9**(3), 205–213 (2010).
2. D. Derkacs, S. H. Lim, P. Matheu, W. Mar, and E. T. Yu, "Improved performance of amorphous silicon solar cells via scattering from surface plasmon polaritons in nearby metallic nanoparticles," Appl. Phys. Lett. **89**(9), 093103 (2006).
3. M. Losurdo, M. M. Giangregorio, G. V. Bianco, A. Sacchetti, P. Capezzuto, and G. Bruno, "Enhanced absorption in Au nanoparticles/a-Si:H/c-Si heterojunction solar cells exploiting Au surface plasmon resonance," Sol. Energy Mater. Sol. Cells **93**(10), 1749–1754 (2009).
4. K. R. Catchpole and A. Polman, "Design principles for particle plasmon enhanced solar cells," Appl. Phys. Lett. **93**(19), 191113 (2008).
5. U. Guler and R. Turan, "Effect of particle properties and light polarization on the plasmonic resonances in metallic nanoparticles," Opt. Express **18**(16), 17322–17338 (2010).
6. M. Schmid, R. Klenk, M. Ch. Lux-Steiner, M. Topič, and J. Krč, "Modeling plasmonic scattering combined with thin-film optics," Nanotechnology **22**(2), 025204 (2011).
7. K. L. Kelly, E. Coronado, L. L. Zhao, and G. C. Schatz, "The optical properties of metal nanoparticles: the influence of size, shape, and dielectric environment," J. Phys. Chem. B **107**(3), 668–677 (2003).
8. K. R. Catchpole and A. Polman, "Plasmonic solar cells," Opt. Express **16**(26), 21793–21800 (2008).
9. R. B. Dunbar, T. Pfadler, and L. Schmidt-Mende, "Highly absorbing solar cells--a survey of plasmonic nanostructures," Opt. Express **20**(S2 Suppl 2), A177–A189 (2012).
10. C. Ciracì, R. T. Hill, J. J. Mock, Y. Urzhumov, A. I. Fernández-Domínguez, S. A. Maier, J. B. Pendry, A. Chilkoti, and D. R. Smith, "Probing the ultimate limits of plasmonic enhancement," Science **337**(6098), 1072–1074 (2012).
11. A. F. Oskooi, D. Roundy, M. Ibanescu, P. Bermel, J. D. Joannopoulos, and S. G. Johnson, "MEEP: A flexible free-software package for electromagnetic simulations by the FDTD method," Comput. Phys. Commun. **181**(3), 687–702 (2010).

#191119 - $15.00 USD Received 24 May 2013; revised 5 Jul 2013; accepted 13 Jul 2013; published 24 Jul 2013

12. S. K. Gray and T. Kupka, "Propagation of light in metallic nanowire arrays: Finite-difference time-domain studies of silver cylinders," Phys. Rev. B **68**(4), 045415 (2003).
13. S. Zhang, K. Bao, N. J. Halas, H. Xu, and P. Nordlander, "Substrate-induced fano resonances of a plasmonic nanocube: A Route to Increased-Sensitivity Localized Surface Plasmon Resonance Sensors Revealed," Nano Lett. **11**(4), 1657–1663 (2011).
14. J. Jung, T. G. Pedersen, T. Søndergaard, K. Pedersen, A. N. Larsen, and B. B. Nielsen, "Electrostatic plasmon resonances of metal nanospheres in layered geometries," Phys. Rev. B **81**(12), 125413 (2010).
15. U. Hohenester and A. Trügler, "MNPBEM – A Matlab toolbox for the simulation of plasmonic nanoparticles," Comput. Phys. Commun. **183**(2), 370–381 (2012).
16. A. Centeno, F. Xie, and N. Alford, "Light absorption and field enhancement in two-dimensional arrays of closely spaced silver nanoparticles," J. Opt. Soc. Am. B **28**(2), 325–333 (2011).
17. T. L. Temple, G. D. K. Mahanama, H. S. Reehal, and D. M. Bagnall, "Influence of localized surface plasmon excitation in silver nanoparticles on the performance of silicon solar cells," Sol. Energy Mater. Sol. Cells **93**(11), 1978–1985 (2009).
18. C. F. Bohren and D. R. Huffman, "Absorption and Scattering of Light by Small Particles" (Wiley-VCH, 2004).
19. A. D. Rakic, A. B. Djurisic, J. M. Elazar, and M. L. Majewski, "Optical properties of metallic films for vertical-cavity optoelectronic devices," Appl. Opt. **37**(22), 5271–5283 (1998).

1. Introduction

The necessity of extending optical path length of light inside a thin-film solar cell device for efficient light absorption by the active material calls for a refined method other than the surface texturing commonly applied in wafer based solar cells. One viable option is to utilize strong plasmonic scattering from metallic nanoparticles (NPs) placed on the front or back surface of the cell [1,2]. It was shown that solar cell efficiency can be improved through increased light scattering into the active part of the device having higher dielectric constant than the surrounding medium, which is air in most of the cases [3]. The path length travelled by the light rays in the device can be increased to an order of 30 times for certain configuration of NPs [1,4]. However, it should be kept in mind that the metal NPs do also introduce losses through absorption of light in the metal rather than the solar cell due to strong coupling of the incident field to the localized surface plasmons (LSPs). Since both absorption and scattering cross-sections are functions of the NP size, yet to a different strength of dependence, for a given metal NP-dielectric medium system a minimum size is found at which scattering cross-section exceeds absorption cross-section of the NP to a significant degree, such that the net effect of presence of the metal NP yields a gain for the solar cell. This competition between absorption and scattering cross-sections was shown to be a strong function of the NP size. Typically, the scattering cross-section can exceed the absorption cross-section for diameters larger than 70 nm in Ag NPs [5,6]. In Ag NP based plasmonic solar cells with NP diameters of about 100 nm, the scattering cross-section surely dominates over the absorption in the entire solar spectrum and this leads to a real gain in the efficiency of the solar cell. The design parameters for such a system should maximize conversion of sun light to photocurrent as much as possible by the solar cell at all frequencies. Metallic NPs show a resonance (plasmon) behavior when it comes to interacting with light [5]. Although plasmons in homogenous media are well understood [7] inhomogeneities caused by substrate interface or influences of other proximate metallic NPs are not so well, yet those play important role in optical response which must be taken into account in order to interpret the experimental data more realistically [8–10]. Our aims are to show how plasmonic resonances are affected by the various inhomogeneities including those originating from the substrate material, submerging behavior of NPs into the substrate and influences of other neighboring particles, and provide insight into how we can positively manipulate these features for improved solar cell applications.

In this work, we compare the experimental results obtained by a series of experiments on plasmonic metal NPs with theoretical results generated by finite difference time domain (FDTD) method. In the experimental part of the study, we produce Ag NPs by dewetting technique on four different substrates, namely Si, SiO_2, Si_3N_4, and InSnO (ITO). We choose these substrates because of their well established use in both crystalline and thin film Si solar cell technologies.

#191119 - $15.00 USD Received 24 May 2013; revised 5 Jul 2013; accepted 13 Jul 2013; published 24 Jul 2013

In the theoretical part, we solve full three dimensional (3D) time dependent electromagnetic wave equation using FDTD method [11] in order to investigate various configurations of metallic NPs with respect to the substrates. FDTD recently has been used in calculation of plasmonic response of complex systems [9,12]. We compare simulation results to experiments by examining the peak resonance positions of comparable size Ag NPs in simulation located at various positions with respect to substrate [13,14]. Our simulation data gives information on whether spherical, hemispherical or spheroid shapes of NPs may have been resulted in the experimental fabrication procedure since dewetting technique relies on self-organized formation of NPs with no external control for precise NP shape.

Although FDTD is a powerful method, for precise description of optical response, its implementation in this kind of analysis tends to be slow due to full propagation of electromagnetic wave equation with very fine mesh requirement inside metallic regions due to high dielectric constant of metal. Therefore, we chose to employ a boundary element method (BEM) [15] for the calculations involving large metallic surfaces as in the case where we studied the interaction among Ag NP spheres. We show that interaction among NPs causes red shifted dipole resonances [16]. This explains that the reason of observed red shifts and wide shoulders in our experimental scattering data due to the dense surface packing in some configurations.

The organization of the paper is as follows: first, we present the experimental details in the following section. Next, we examine the important effects observable in a homogenous medium. Then, we discuss inhomogeneous medium effects such as NP and substrate interface and the interactions of NPs in the close vicinity of another NP. We conclude with a discussion and summary section.

2. Experimental results

We studied the effects of substrates with technological interest for solar cell industry on the plasmonic properties Ag NPs fabricated by dewetting technique. Four different substrates, namely Si, SiO_2, Si_3N_4, and InSnO (ITO), were chosen as substrates because of their importance in both crystalline Si and thin film solar cell technologies. Moreover, these substrates provide a good variety of electrical and thermal conductivities which are related to their optical properties.

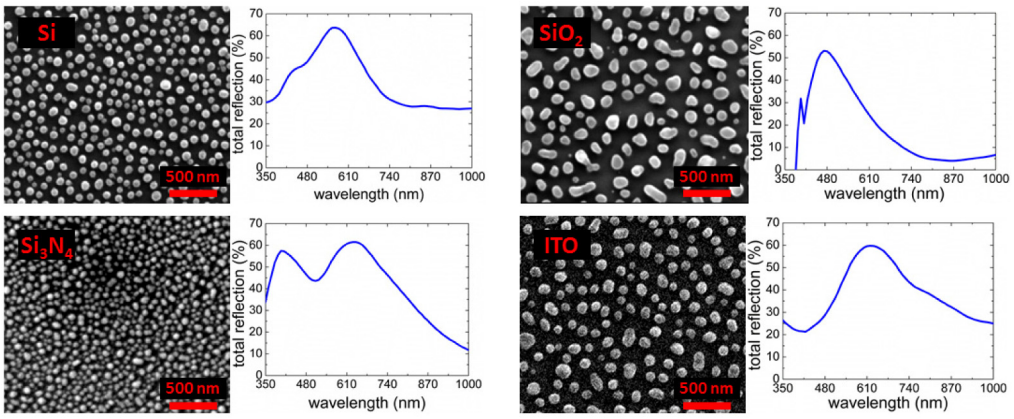

Fig. 1. The SEM images and the corresponding measured total reflection data of Ag NP decorated Si, SiO_2, Si_3N_4, and ITO surfaces by dewetting method.

For all substrates used in this work, initially 12 nm Ag thin films were coated on the surface of the samples by thermal evaporation under 4-5 × 10^{-6} Torr base pressure and with a rate of 0.5 Å/sec. Then, in order to trigger the NP formation, samples were annealed at 400 °C for an hour in a tube furnace under N_2 flow with a rate of 150 sccm. The samples were imaged by SEM (FEI Quanta 400F). A representative SEM image in a proper magnification

#191119 - $15.00 USD Received 24 May 2013; revised 5 Jul 2013; accepted 13 Jul 2013; published 24 Jul 2013

was used for comparison between the particles on different surfaces. The totally back-scattered photons (total reflectance), comprised of both the specular and the diffuse reflection from the sample surface were measured using an integrating sphere (Oriel) coupled to a monochromator (Oriel). The raw data were processed with respect to a calibration disc which provides a 100% reflective surface.

Figure 1 shows the SEM images and the total reflectance data of the Ag NPs formed on these 4 substrates at the dewetting temperature of 400 °C. In reflectance measurements, the light that is forward-scattered (transmitted into the active region of the substrate) or that is absorbed by the Ag NPs is not to be detected, resulting in a reduction of reflectance. However, the light that is back-scattered (reflected) by the Ag NPs will be detected, resulting in an elevated reflectance. It is remarkable that the Ag NPs act as an anti-reflection coating for two different regimes, namely mostly in UV (350-400) and in NIR (>700 nm) parts of the spectrum for all of the substrates, but tend to increase the reflectance at the dipolar resonance [17]. The same experiment was repeated and a set of optical data were generated for different annealing temperatures. A more detailed analysis of formation kinetics as well as optical spectra as a function of the process temperatures are discussed in a separate publication. Here, we focus on the representative optical data and their theoretical description using FDTD and BEM. We see that both the Ag NP mean size and its size distribution are greatly influenced by the type of the underlying substrate.

3. Theory: homogenous medium

It is known that plasmonic behavior of metal NPs is very sensitive to the dielectric properties of the local environment. This sensitivity can be predicted from the solution of the Maxwell's equations that give a direct dependence of resonance condition on the dielectric constant of the surrounding environment. Plasmon resonance of Ag nano-spheres inside homogeneous medium can be calculated exactly using Mie theory [18]. Even though, the extensions to spheroids are also possible [7], for predicting the behavior of systems with inhomogeneous medium or shapes, other approaches are required.

Dewetting based fabrication results in a nanoparticle population with non-uniform size and shape. We observe different plasmonic response for 4 different substrates. Therefore, we first solve Maxwell's equations in a homogenous environment and discuss these effects regarding our experimental results.

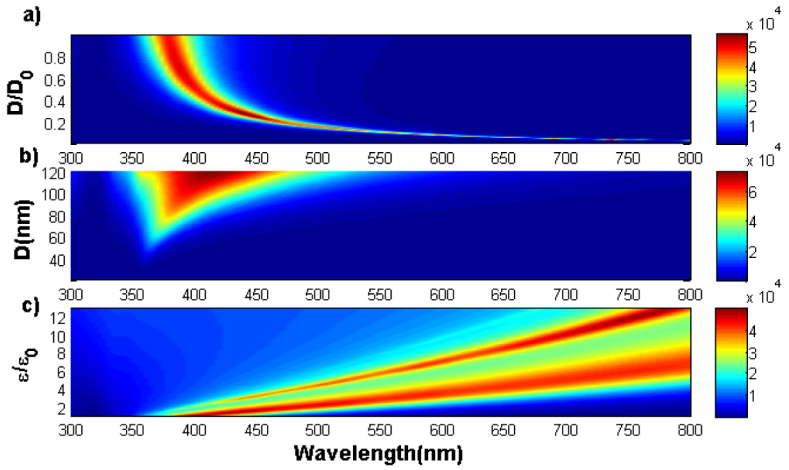

Fig. 2. (a) The scattering cross section for a prolate spheroid. Principal axis ratio is defined for the starting Ag sphere with diameter D_0 = 100 nm. (b) Scattering cross section as size of Ag sphere changes in homogenous medium of air. (c) Scattering cross section as the homogenous medium dielectric constant changes for an Ag sphere of diameter D = 100 nm.

#191119 - $15.00 USD Received 24 May 2013; revised 5 Jul 2013; accepted 13 Jul 2013; published 24 Jul 2013

In Fig. 2, we show plasmonic behavior of Ag NPs inside a homogeneous medium calculated using exact Mie theory. In Figs. 2(a) -2(c), we plot the scattering cross section in units of (nm^2) color coded with color intensity meter shown in rectangular boxes next to each plot. In Fig. 2(a), we show effect of shape by changing one of the principal axes of sphere. As the shape goes from sphere to a prolate shape plasmon resonance red shift. In SEM images, in most cases we have an oblique view of Ag NPs. We believe that most of the particles are not perfect spheres but prolate shape. The main effect of this distortion is red shifting of plasmon frequency and diminishing higher order excitations. We will discuss more about this later taking into account interactions. In Fig. 2(b), we show size dependence. The scattering cross section is only effective when pass a critical radius, at around diameter, D = 70 nm, scattering cross section becomes dominant. This was previously predicted by a simple model based on Discrete Dipole Approximation (DDA) [5]. Moreover, for small radius spheres, absorption due to sphere leads to heat dissipation and not useful in solar cell applications. In Fig. 2(c) we show the effect of homogenous medium. As the dielectric constant of medium increases plasmon frequency red shifts and higher order modes, i.e. quadrupole, octupole moments will appear. We further discuss this feature in the next section when we have Ag NPs at interface of air and dielectric semiconductor.

4. Theory: inhomogeneous medium

More interesting is the behavior of Ag NPs in inhomogeneous medium. In almost all cases we want NPs near or inside a semiconductor interface. This is an important design parameter for solar cell application. To understand the variations with inhomogeneous environments, we have carried out experiments and theoretical calculations based on FDTD approach [11].

In order to simulate Ag material for such purpose in our simulations, Drude-Lorentz fit of the data taken from Palik's book, Drude and additional 5 Lorentzian terms, is adapted into MEEP's Lorentzian terms [19]. We have a relative error of 1% with respect to the exact result from Mie calculation for a mesh size of 200 × 200 × 200. A typical run takes 12 hours of CPU time by using an 8 core workstation to complete, which at the end produces the scattering cross section of NPs over a range of wavelengths.

4.1 Interaction with substrate

We conduct numerical simulations of Ag NPs at the interface of semiconductor and air to compare with experimental result. We run likely scenarios numerically and compare to experimentally obtained peak positions.

A typical simulation run is shown in Fig. 3 for ITO substrate. We show plasmonic response for four different locations of Ag NPs relative to the substrate as depicted in insets in Figs. 3(a) –3(d). We model the interaction of a single NP with substrate so we use a perfectly matching boundary condition in all calculations instead of periodic boundary conditions. This is not a good representation of the experimental situation, but we would like to separate the effects of particle-particle interactions and particle-substrate interaction and we focus our attention to the regions on solar cells where the effect of nearby particle can be considered as not important. We consider the effect of particle-particle interaction separately in the next section. We looked at a modified substrate model in Fig. 3d where we extended the substrate in x-y plane and negative z direction. We observe not many differences in scattering efficiency peak positions. In the insets of Figs. 3(a) -3(c), we show a 2D projected view of typical calculation geometries for the simulations. Computational cell is chosen such that as the outermost box corresponds to $600 \times 600 \times 600\, nm^3$. A source which is located near the top surface produces a Gaussian wave pulse of y polarized electric field. We calculate the Poynting vector at the surface of an imaginary box of $350 \times 350 \times 350\ nm^3$ shown as red rectangular region with and without the Ag NP in the system. In each case two runs are necessary to find the difference of powers due to the inclusion of Ag NPs. We need this normalization since we are interested in the scattering power of Ag NPs and not the substrate. Total power on the surface of imaginary box is calculated by

#191119 - $15.00 USD Received 24 May 2013; revised 5 Jul 2013; accepted 13 Jul 2013; published 24 Jul 2013

$$P(\omega) = \mathrm{Re}\left(n \cdot \oint E_{\omega}(x) \times H_{\omega}(x) da\right), \tag{1}$$

which can be used to calculate scattering cross section as

$$C_{sca}(\omega) = \frac{P(\omega)}{I(\omega)}, \tag{2}$$

where $\hat{n}$ is the outward normal direction to the surface, ω indicate the frequency and $I(\omega)$ is the intensity of light source in units of power per unit area. For some simple geometries it is possible to define the scattering efficiency as the ratio of scattering cross section to the geometric cross section, $\sigma_{sca} = C_{sca} / A$, where A is the physical cross section of Ag NP perpendicular to the direction of incident light. We report our result in terms of scattering efficiency as it is possible to find an effective geometric cross section for the spheres.

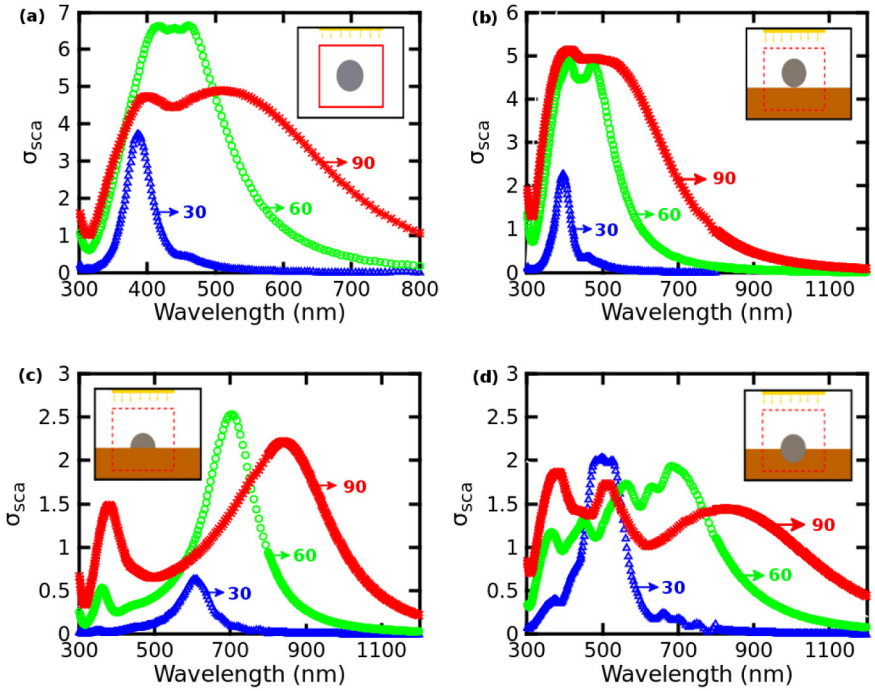

Fig. 3. Various positions of Ag nano sphere (sphere radius = 30 nm – blue triangles, 60 nm – green spheres, 90 nm – red stars) and ITO film. (a) Ag nano sphere is in Air (b) Ag nano sphere is on ITO film (c) Ag nano hemi-sphere is on ITO film (d) Ag nano sphere is immersed in ITO film.

We see that the plasmonic scattering spectrum is greatly influenced by the contact area and geometry of the interface. We observe an increase in the amplitude of the dipole peak (second peak at 500 nm) in Figs. 3(a) and 3(b) as the contact area between nano sphere and underlying dielectric slab increases. We typically see 2 distinct plasmon peaks at corresponding wavelengths as if the sphere were entirely in air and in semiconductor. In the experiment, however, we do not observe the peak corresponding to air medium most likely due to insensitivity of detectors at low wavelengths and the low relative intensity.

In Fig. 4, we show the comparison between experimental data and theoretical plasmon resonances calculated for a series of realistic conditions. The experimental data were obtained from the samples annealed at different temperatures. It is observed that changing the annealing temperature strongly affects the average particle sizes and causes non-spherical (worm-like) shapes of particles. Peak positions of reflectance measurements, as indicated in

#191119 - $15.00 USD Received 24 May 2013; revised 5 Jul 2013; accepted 13 Jul 2013; published 24 Jul 2013

Fig. 1, on different sets of samples are compared with the simulation results. We see that the plasmon peaks shift to red with increasing particle size as predicted by the theoretical calculations. In order to match the theoretical data to the experimental one, three different conditions are taken into the account: the Ag NP is a sphere touching the surface at one point, or a hemisphere with a large interacting interface with the substrate, or entirely immersed sphere into the substrate. We see that our theoretical results approach the experimental data reasonably well in all cases when all three configurations are considered. This is reflecting the inhomogeneous nature of the Ag particle formation by dewetting. However, in the case of Si and SiO_2 substrates, we see better agreement with one configuration only, indicating a more homogenous distribution. The SEM pictures shown in Fig. 1 are indeed showing a more uniform distribution of Ag NPs for these two substrates.

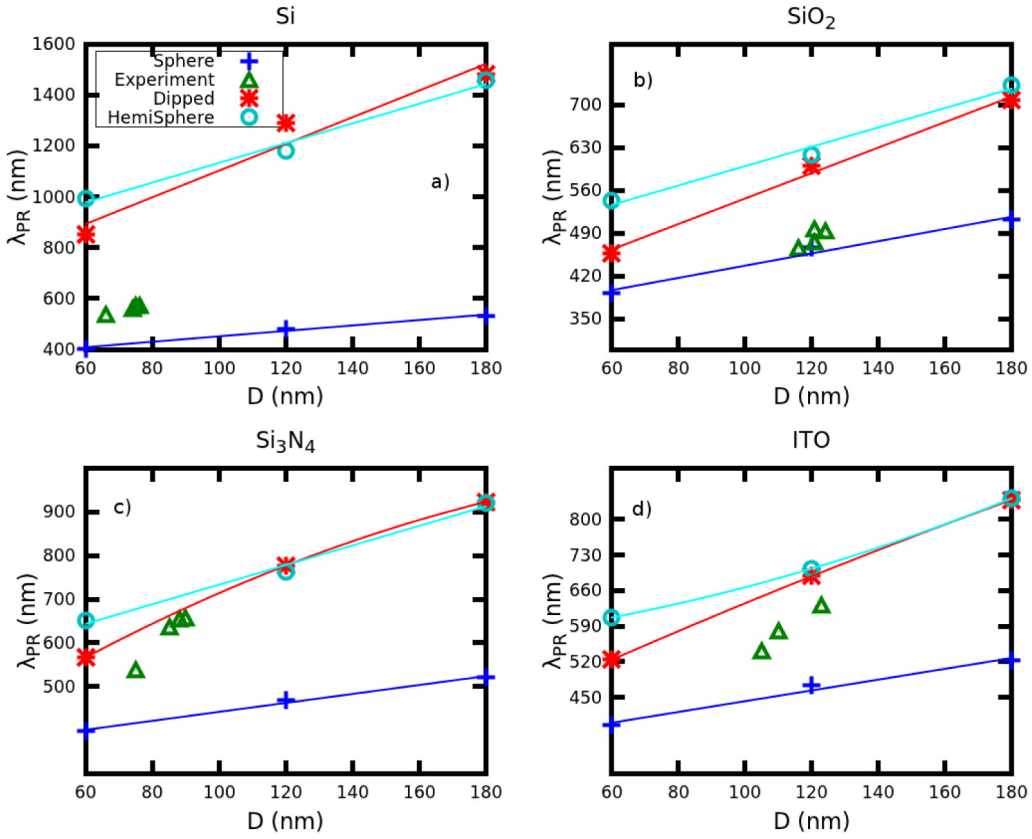

Fig. 4. Experimental and theoretical plasmon resonance changes as a function of NP diameter placed in (a) Si medium (b) SiO_2 medium (c) Si_3N_4 medium (d) ITO medium. Different symbols show different NP locations.

The inset of left panel of Fig. 5 displays an SEM image of Ag decorated ITO surface produced by surface dewetting of originally 12 nm thick Ag thin film by 300°C annealing under N_2 flow for 1 hour. The size distribution of Ag NPs on this surface is calculated using an image analysis software (Gwyddion) and the particle size distribution is given as a histogram in the left panel of Fig. 5. The histogram shows a mean radius of 55 nm which corresponds to a 110 nm NP average size. The FWHM of size distribution is roughly 60 nm. In the right panel of Fig. 5, red curve displays experimentally measured scattering efficiency by integrator based reflectance setup. In addition, along with the measured curve, the FDTD result of one quarter immersed spherical Ag NP with radius 60 nm on ITO surface is plotted the right panel of Fig. 5. The qualitative agreement of the disappearance of quadrupole peak

#191119 - $15.00 USD Received 24 May 2013; revised 5 Jul 2013; accepted 13 Jul 2013; published 24 Jul 2013

and the peak position of the observed resonance suggests that the Ag most likely did not completely dewet the ITO surface but an immersed or hemispherical NP is formed.

4.2 Interaction among particles

In experiments, we observe inhomogeneous distribution of particles which suggests that the interactions among them are likely an important parameter for understanding the overall plasmonic response. We test this by solving full electromagnetic wave equation using BEM [15]. The relative cross section enhancements as high as 10 means that it is sufficient to cover 10 percent (although we have about 40% in ITO substrate and changes around that for the other substrates in our experiments) to have the maximum benefit of plasmonic light scattering into the active medium of the thin film solar cell device. In general, there may be more than two particles that come close to each other and start to interact. This makes linear averaging of cross sections not a plausible method to understand the overall behavior due to modified scattering cross sections in interacting Ag NPs.

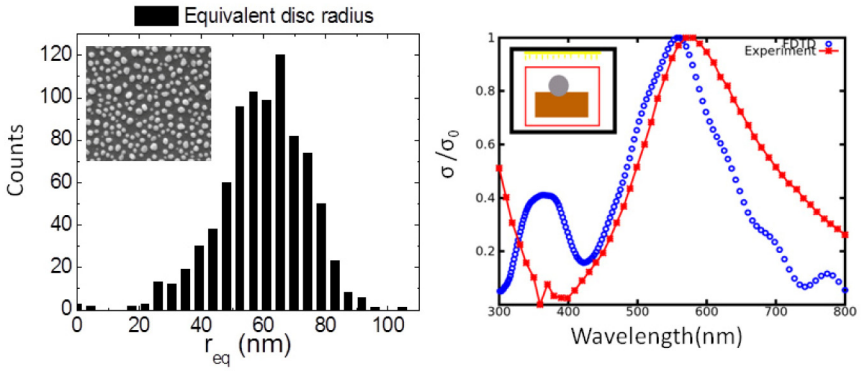

Fig. 5. The size distribution of Ag NPs on ITO surface is shown on the left. Inset displays the SEM image of it. On the right, the measured and the FDTD calculated scattering efficiencies are presented.

In Fig. 6, we show the effect of interaction on the plasmon resonance for Ag nano spheres in air. We use a unit cell of 3 equal size spheres in an L shaped configuration with the two outlying spheres located at the same distance to the central one. This configuration is particularly beneficial in our calculations as we would like to get a general idea about the three particle response independent of the incident polarization. Different curves in Fig. 6 correspond to the distances, L, between neighboring two spheres along x and y directions changed by the same amount. We find out that as the two spheres come close to the central one, there is a red shift of dipole resonance while quadrupole resonance remains at its original place. This is indeed the case in the experiment. For instance in Fig. 1(c) we show data for Ag NPs on silicon nitride substrate. This is the setup where surface coverage is much higher than other substrates. We observe a double peak suggesting that a red shift happens due to the interaction of the particles in that system. In Fig. 6, we also show the surface charge distribution on spherical NPs when the NPs come very close to each other. The surface charge distribution at the resonance positions for L = 2 nm case is depicted as coloring on the sphere surfaces. We see that the dipole resonance at $\lambda = 664$ nm is no longer due to the oscillation of electrons between the two ends of a sphere (which is the case for a single sphere at $\lambda = 395$ nm) but actually between two neighboring spheres, and therefore its position is lower in energy which is the reason of red shift of dipole excitation. Another resonance occurs at $\lambda = 324$ nm again between two neighboring spheres in the form of a quadrupole moment. In Fig. 6, at $\lambda = 303$ nm, we see that the resonance is of quadrupole nature as in that of a single sphere, and at $\lambda = 296$ nm an octupole excitation can be observed as well.

#191119 - $15.00 USD Received 24 May 2013; revised 5 Jul 2013; accepted 13 Jul 2013; published 24 Jul 2013

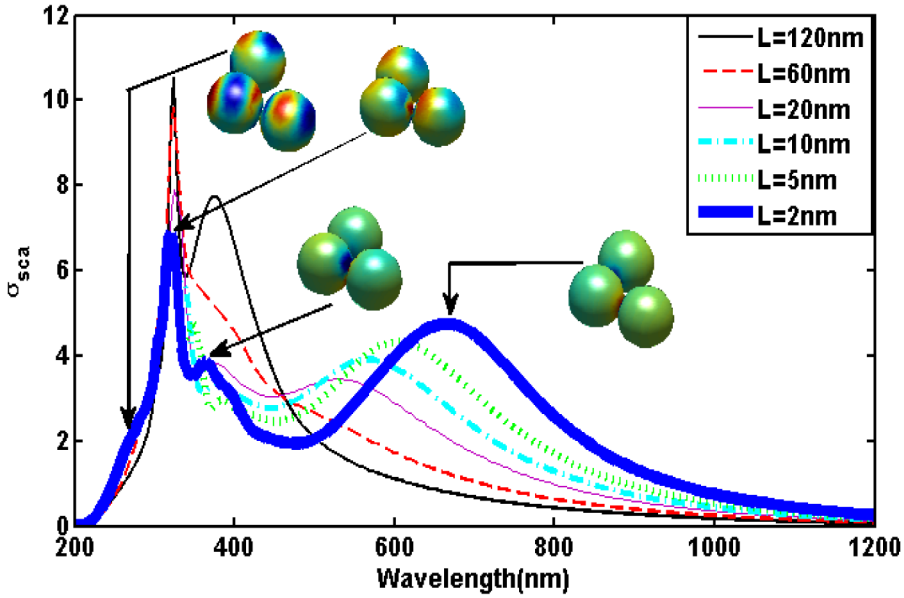

Fig. 6. Interaction of three similar sized Ag NPs with each other.

5. Discussion and conclusions

Engineering the necessary conditions for better light trapping by plasmonic nanostructures in order to achieve improved conversion of light into photocurrent is both an academic and technologically important challenge especially for new generation of thin film solar cell applications. In order to attempt engineering such plasmonic interfaces, it is of importance to first have a detailed understanding of the mechanisms of interaction of light with the plasmonic and dielectric counterparts. The most preferable strategy of integration of plasmonic interfaces with full-scale solar cell devices are bottom–up approaches such as self-organized dewetting based fabrication techniques as the difficulty of uniform fabrication procedures and their costs of top-down approaches still remain to be prohibitively high. Nevertheless due to the stochastic nature of dewetting based plasmonic particle decoration, there is little, if not zero, control on the final configuration of plasmonic interfaces produced by this method. Although self-organized methodology is a promising option for production of full-scale plasmonic solar cells, the single NP versus dielectric surface based theoretical models are often found not to be sufficient to describe the intricate relationship of light trapping efficiency of such experimentally attainable surface decorations of this film solar cells. In order to understand the optical properties of such mostly randomly configured nanoparticle network on dielectric surfaces, we believe that it is important to take into account usually ignored properties of NPs such as: their shapes to be often deviating from ideal spheres to prolate and oblate spheroids; their nature of being floating on or immersed into the underlying dielectric film; and their mutual interactions including more than two particles. In this work, we deal with practical means of endeavoring such an initiative. We show experimentally the possibility to scatter light from Ag NPs preferentially into an underlying transparent conductive oxide (TCO) material (ITO in this case) and thereby effectively increasing the number of photons interacting with the active layers of the device for improved efficiency, in a way like an anti-reflection coating would do. We explain the origin of this scattering mechanism by showing plasmonic response of the Ag NPs and their various interactions with the semiconductor thin film and other NPs in the vicinity. Five categories of parameters, namely, shape, size, medium, medium discontinuities and inter-particle interactions have been discussed to interpret the experimental data. The main parameter of interest is the plasmonic resonance peak position since its position determines

#191119 - $15.00 USD Received 24 May 2013; revised 5 Jul 2013; accepted 13 Jul 2013; published 24 Jul 2013

the energies of incident light that is scattered most efficiently. In thin film solar cells such Ag NPs can be incorporated as efficient back reflectors as they would back scatter the incoming radiation very strongly into the solar cell layers at their plasmonic resonances. The Fig. 2 suggests that by targeting a particular average size and by carefully choosing the layer into which such NPs would be embedded depending on the layers dielectric function, a certain wavelength range can be targeted. It is remarkable that Ag originally having bulk plasmon resonance at as low as 350 nm can be tailored to have very strong multipole resonances at wavelengths reaching 750-800 nm where a strong back scattering of the radiation in to Si based active layers would be most beneficial. We find that shape and the degree of Ag NP immersion inside the thin film can also be a control parameter to manipulate the resonance spectrum and thereby the optical path length improvement in TCO especially when a broad-band application is required. It is expected that resulting geometries of hemispherical Ag NPs or immersed Ag NPs of 90 nm or higher results in a response which is as broad as to cover the entire Si absorption band of 400-1100 nm. Finally, a red shift of plasmon frequency is observed when NPs are brought close to each other as well as when they are immersed in high index semi-medium. This effect can readily be experimentally confirmed on the densely packed Si_3N_4 substrate and is in general agreement with observed wide peak shoulder towards high frequency in experimental scattering data. It should be noted that even with the self-organized fabrication technique of dewetting, the plasmonic interfaces can be steered to attain the beneficial properties by using a few free fabrication parameters such as temperature and substrate choice. By using our findings on shape, size, medium, medium continuity and interparticle interactions, these plasmonic interfaces can be tailored to act most efficiently at especially difficult to trap longer wavelengths of solar radiation in thin films for improved solar cell devices.

Acknowledgments

We acknowledge support from the Scientific and Technological Research council of Turkey (TUBITAK) grant number 109R037, joint project with BMBF, Rainbow Energy. The research leading to these results has received funding from the European Union's Seventh Framework Programme FP7/2007-2013 under grant agreement n° 270483 and Middle East Technical University BAP-08-11-2011-129 grant.

#191119 - $15.00 USD Received 24 May 2013; revised 5 Jul 2013; accepted 13 Jul 2013; published 24 Jul 2013